UV-curable thiol-ene networks with intrinsic antioxidant functionality from eugenol-derived triallyl isocyanurate

Reactive and Functional Polymers 222 (2026) 106701

Contents lists available at ScienceDirect

Reactive and Functional Polymers

journal homepage: www.elsevier.com/locate/react

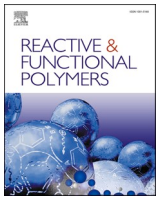

UV-curable thiol-ene networks with intrinsic antioxidant functionality from eugenol-derived triallyl isocyanurate

Mohamed Naguib [a,b], Marco Sangermano [c], Mohamed A. Yassin [a,d,*]

[a] Chemical Industries Research Institute, National Research Centre, 12622 Giza, Egypt
[b] Academy of Scientific Research & Technology (ASRT), 101 Kasr Al-Ainy St, Cairo, Egypt
[c] Dipartimento Scienza e Tecnologia dei Materiali (DISAT), Politecnico diTorino, Torino, Italy
[d] Leibniz-Institut für Polymerforschung Dresden e.V., 01069 Dresden, Germany

ARTICLE INFO

Keywords:
Bio-based polymer
Eugenol
Isocyanurate
Thiol-ene networks
Antioxidant
UV-blocking

ABSTRACT

The development of bio-based polymers with intrinsic antioxidant functionality offers a sustainable strategy to enhance material longevity and stability while reducing reliance on migratory additives. Herein, a triallyl isocyanurate monomer (TEG) was synthesized via the reaction of eugenol, a renewable phenolic compound, with thermally stable hexamethylene diisocyanate isocyanurate. TEG was subsequently employed to construct functional thiol-ene networks through UV-initiated thiol-ene photopolymerization with multifunctional thiols. Additional formulations incorporating pristine eugenol were designed to preserve pendant phenolic hydroxyl groups, thereby imparting enhanced radical-scavenging capacity. The photopolymerization kinetics, monitored by real-time FTIR and photo-DSC, revealed rapid curing with high thiol conversion (≈78%) achieved within 2 min of irradiation. A slight retardation (conversion ≈72%) was observed in systems containing pendant phenolic hydroxyl due to their free radical quenching effect. Dynamic mechanical analysis confirmed that increasing thiol functionality led to higher crosslink densities and elevated glass transition temperatures (T_g = 16–38 °C), while tensile testing demonstrated tunable stiffness (E_t = 1.2–54.3 MPa) and elongation (ε_M = 47–63%). The resulting networks exhibited excellent optical transparency (>80% transmittance at 500 nm), effective UV-shielding (~0% transmittance below 320 nm), and outstanding thermal stability (T_{max} ≈ 320 and 460 °C). DPPH assay verified strong intrinsic antioxidant activity especially for phenolic hydroxyl containing formulations, achieving up to 86% radical scavenging. Collectively, these findings establish a sustainable design approach for multifunctional thiol-ene networks that unite mechanical adaptability, UV protection, thermal robustness, and built-in antioxidant functionality, suitable for applications in flexible coatings, packaging, and protective materials.

1. Introduction

Intrinsic antioxidant polymers, unlike conventional additive-based systems, represent a class of materials in which antioxidant moieties are covalently or physically integrated into the polymer backbone or network structure [1,2]. This integration offers distinct advantages over the simple blending of small-molecule antioxidants, including reduced migration, prolonged functional lifetime, and enhanced oxidative stability [3]. Consequently, intrinsic antioxidant systems have gained considerable attention for use in advanced coatings, biomedical devices, and high-performance polymeric materials where long-term durability and safety are paramount. A wide range of chemistries has been explored for designing such systems, particularly those incorporating hindered phenolic groups capable of radical scavenging and stabilization [4,5].

Parallel to this development, growing emphasis on sustainability has driven the design of bio-based antioxidant polymers incorporating naturally derived moieties such as vanillin [6,7] and lignin derivatives [8]. Among these, eugenol, a naturally occurring phenolic compound predominantly obtained from clove oil, has emerged as a versatile renewable feedstock. Its aromatic ring, allylic double bond, and phenolic hydroxyl group offer multiple reactive sites, enabling diverse chemical modifications and integration into polymeric architectures [9–12]. Eugenol-based monomers have been successfully employed in various polymer systems, imparting desirable characteristics such as rigidity, thermal stability, UV-absorption, and antioxidant. Recent

* Corresponding author at: Leibniz-Institut für Polymerforschung Dresden e.V., 01069 Dresden, Germany.
E-mail address: Yassin@ipfdd.de (M.A. Yassin).

https://doi.org/10.1016/j.reactfunctpolym.2026.106701
Received 27 November 2025; Received in revised form 30 January 2026; Accepted 14 February 2026
Available online 17 February 2026

examples include tri-epoxidized eugenol for bio-based epoxy resins [13], Eugenol-based monomers containing phosphorous for flame retardant thiol–ene networks [14–17], and fully bio-based diallyl monomers derived from eugenol and itaconic acid for thiol-ene systems [18].

Polyurethanes constitute one of the most versatile polymer families, widely utilized in foams, durable elastomers, protective coatings, and flexible adhesives owing to their tunable mechanical and thermal properties [19,20]. The development of bio-based polyurethanes has attracted significant interest as a sustainable alternative to petroleum-based analogues [21–24]. Incorporation of isocyanurate units, formed via isocyanate cyclotrimerization, further enhances the chemical resistance, thermal stability, and flame retardancy of polyurethane materials, making isocyanurate-containing systems attractive for high-performance applications [25–27].

Thiol-ene networks, formed through the highly efficient "click" reaction between multifunctional thiols and alkenes, offer a robust platform for constructing crosslinked polymers with precise architecture and excellent property control [12,28,29]. These reactions, typically initiated by UV light, proceed rapidly under mild conditions and exhibit minimal oxygen inhibition, low polymerization shrinkage, and uniform network formation. As a result, thiol-ene systems have found extensive use in advanced manufacturing, including high-resolution 3D printing [30,31], optical lenses, biomedical materials [32], and functional coatings [33,34].

In this study, bio-based thiol-ene polyurethane networks incorporating eugenol as a renewable phenolic building block are developed to achieve materials with tailored mechanical properties, enhanced thermal stability, and intrinsic UV-blocking and antioxidant functionality. A triallyl isocyanurate derivative (TEG) is synthesized via the reaction of eugenol with hexamethylene diisocyanate isocyanurate (HDI-trimer), followed by UV-initiated thiol-ene photopolymerization with tri- and tetra-functional thiol crosslinkers. Selected formulations are deliberately designed to preserve free phenolic hydroxyl groups from eugenol, imparting radical-scavenging capability while maintaining network integrity. The study systematically investigates the synthesis, reaction kinetics, and structure property relationships of the resulting networks, including their viscoelastic behavior, mechanical performance, optical transparency, thermal stability, UV-shielding ability, and antioxidant activity. Collectively, this work establishes a sustainable design approach for multifunctional eugenol-based thiol-ene networks that integrate structural versatility with multifunctionality, offering potential applications in flexible coatings, biomedical devices, food packaging, and protective materials.

2. Experimental section

2.1. Materials

Eugenol (EG), trimethylolpropane tris(3-mercaptopropionate) (3SH), pentaerythritol tetrakis(3-mercaptopropionate) (4SH), Dibutyltin dilaurate 95% (DBTDL), 2,2-Diphenyl-1-picrylhydrazyl (DPPH) and phenylbis(2,4,6-trimethylbenzoyl)phosphine oxide 97% (BAPO) were purchased from Merck. Hexamethylene diisocyanate isocyanurate (HDI-trimer), commercially available under the trade name *POLURGREEN MT 100 LV 01* (NCO content: 22–23%), was kindly supplied by SunChemical, Italy.

2.2. Preparation of tri-eugenol based isocyanurate (TEG)

The tri-eugenol based isocyanurate was synthesized as shown in Scheme 1. Eugenol and HDI-isocyanurate trimer were reacted at an equimolar ratio of NCO:OH (1:1) in THF at 50 °C under nitrogen atmosphere, using DBTDL (0.01 wt%) as a catalyst. Reaction progress was monitored by ATR-FTIR through observation of the gradual decrease in the intensity of the characteristic NCO absorption band at 2260 cm^{-1}. Upon completion, THF was removed under reduced pressure to obtain TEG as a viscous liquid with a conversion of approximately 95%.

2.3. Preparation of biobased thiol-ene networks

Four thiol-ene formulations were prepared using TEG (a triallyl monomer), either individually or in combination with eugenol (a monoallyl monomer), together with two multifunctional thiol crosslinkers (3SH and 4SH), as illustrated in Scheme 2. In all formulations, the molar ratio of allyl double bonds to thiol groups was maintained at 1:1. Photopolymerization was initiated by adding BAPO (1 wt%) as photoinitiator. The resulting mixtures (compositions summarized in Table 1) were homogenized, poured into silicone molds, and subsequently cured under UV irradiation (456 mW cm^{-2}, Dymax ECE Flood Lamp, Dymax Europe GmbH, Wiesbaden, Germany) for 120 s.

2.4. Characterization

NMR spectra were recorded on a Bruker Avance III 500 spectrometer operating at 500.13 MHz for ^{1}H and at 125.77 MHz for ^{13}C at 30 °C. The spectra were referenced to the residual solvent signals ($CDCl_3$: $\delta(^{1}H) = 7.26$ ppm, $\delta(^{13}C) = 77.0$ ppm. The NMR spectra were recorded by using the standard Bruker pulse programs.

Fourier-transform infrared (FTIR) spectra were collected using a Nicolet iS10 spectrometer equipped with a diamond crystal in attenuated total reflection (ATR) mode. ATR-FTIR was employed to monitor the conversion of isocyanate groups by tracking the characteristic NCO absorption band at 2260 cm^{-1}, with the C—H stretching region (3100–2800 cm^{-1}) serving as the internal reference.

Photopolymerization kinetics of the four formulations were studied in transmission mode and the UV-curing was performed using a Hamamatsu LIGHTINGCURE LC8 (365 nm, 456 mW cm^{-2} at 80% intensity), with light directed on the sample by an optical fiber. In details, the formulations were applied onto silicon wafer substrate via 12 μm hand coater, and FTIR spectra were recorded at different curing times (0, 10, 20, 30, 60, 90, and 120 s). To improve accuracy, each measurement was performed in triplicate, and the data were processed using Omnic software (Thermo Fisher Scientific). The conversion was calculated according to Eq. (1), based on the decrease in the integral area of S—H stretching band (A_{SH}) at 2570 cm^{-1}, normalized against the integral area of N—H stretching band at 3350 cm^{-1} (A_{ref}). [35]

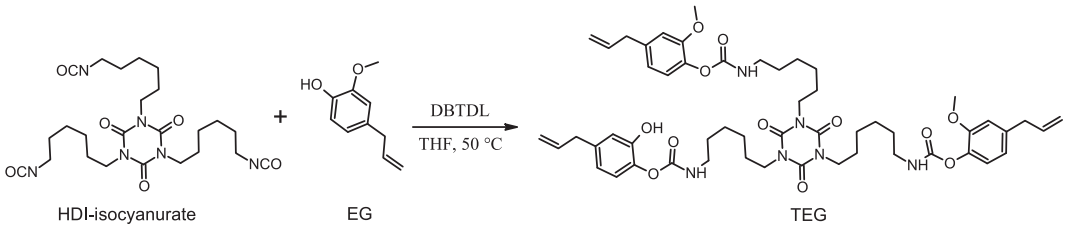

Scheme 1. Synthesis of tri-eugenol based isocyanurate (TEG).

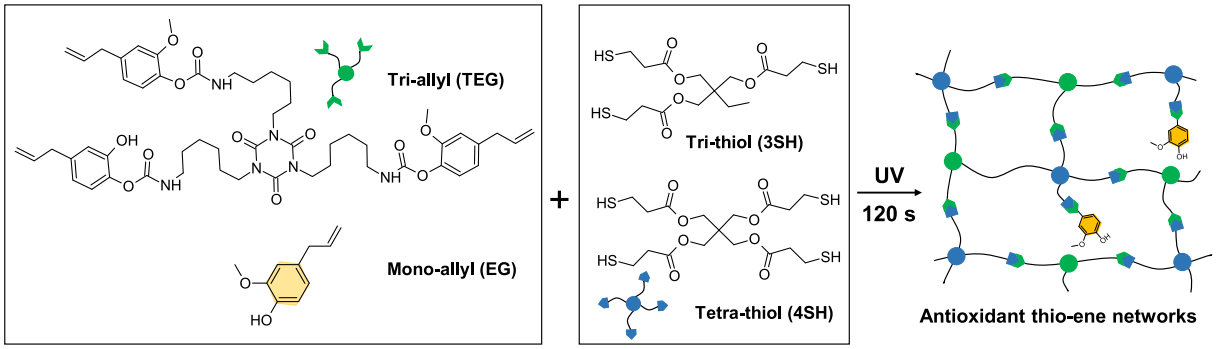

Scheme 2. Formation of TEG-based antioxidant networks via thiol-ene reaction.

Table 1
Compositions of the TEG-based thiol-ene networks. Values represent the molar equivalents of each component.

Entry	EG	TEG	3SH	4SH
TEG-3SH	0.00	1.00	1.00	0.00
TEG-4SH	0.00	1.00	0.00	1.00
TEG-EG-3SH	0.33	0.67	1.00	0.00
TEG-EG-4SH	0.25	0.75	0.00	1.00

$$Conversion, \% = \frac{\left(\frac{A_{SH}}{A_{ref}}\right)_{t=0} - \left(\frac{A_{SH}}{A_{ref}}\right)_{t=x}}{\left(\frac{A_{SH}}{A_{ref}}\right)_{t=0}} \times 100 \quad (1)$$

where A_{SH} and A_{ref} represent the integral areas of the thiol (S—H) band and the reference (N—H) band, respectively, in the spectra under investigation.

Photo-differential scanning calorimetry (Photo-DSC) was performed using a Mettler-Toledo DSC-1 equipped with GC100 gas-controller and a mercury Hamamatsu LIGHTINGCURE LC8 lamp (365 nm, Hamamatsu Photonics) coupled with an optical fiber. Measurements were conducted at 80% light intensity (456 mW cm^{-2}). Approximately 8 mg of each sample was placed in an open 40 μL aluminum crucible, and the analyses were performed in isothermal mode (25 °C) under a nitrogen flow rate of 40 mL min^{-1}. The method consisted of two irradiation phases (120 s each), preceded by 120 s with the lamp switched off. To eliminate non-intrinsic noise, the second exposure curve was subtracted from the first. Data acquisition and processing were performed using Mettler Toledo STARe software.

For DSC measurements, samples (5–10 mg) were sealed in 40 μL aluminum pans and analyzed under nitrogen. The temperature was ramped from −40 to 120 °C at 10 °C/min followed by a cooling ramp from 120 to −40 °C at 10 °C/min. A subsequent second heating cycle was recorded from −40 to 120 °C at 10 °C/min.

Thermogravimetric analysis (TGA) was conducted on a Thermobalance Q5000 (TA Instruments, Waters). The temperature was elevated from room temperature to 700 °C at a heating rate of 10 °C/min. Measurements were performed under a N_2 atmosphere with a mass flow of 50 mL/min.

Dynamic mechanical analysis (DMA) was performed on Triton Technology instrument. The UV-cured samples with average dimensions of 15 × 7 × 0.8 mm were analyzed from −60 °C to 100 °C at a frequency of 1 Hz and a heating rate of 3 °C/min. The glass transition temperature, (T_g) was detected as the peak maximum of tan δ curve. The storage modulus (E') was used to determine the crosslink density (ν) according to Eq. (2) [18].

$$\nu = \frac{E'}{3RT} \quad (2)$$

where E' is the storage modulus in the rubbery plateau (T_g + 40 °C), R is the gas constant and T is the absolute temperature.

Gel content was determined by Soxhlet extraction in THF at 70 °C for 24 h. Then, the insoluble polymers were dried under vacuum at 70 °C for 48 h until a constant weight was achieved. The gel content was calculated according to Eq. (3).

$$\text{Gel content } (\%) = \frac{m_i - m_f}{m_i} \text{ x } 100 \quad (3)$$

where, (m_i) and (m_f) are the initial and final mass of the tested sample, respectively.

The optical transmittance of the UV-cured thiol-ene films was measured using a UV–Vis spectrophotometer (Specord® 210 Plus, Analytik Jena, Germany). The polymeric films were mounted in a film holder, and their transmittance was recorded over the wavelength range of 200–800 nm.

Mechanical properties: Uniaxial tensile tests were conducted on S2-type dumbbell-shaped specimens in accordance with ISO 527-2/5B/1–10 using a universal testing machine (Zwick GmbH & Co. KG, Ulm, Germany) equipped with a Multisens extensometer and a 100 N load cell. Tests were performed at a crosshead speed of 5 mm/min. Reported values represent the mean of six specimens. The elastic modulus (E) was measured at a crosshead speed of 5 mm/min.

Antioxidant assay: The radical scavenging activities of the UV-cured thiol-ene films were investigated using the DPPH assay by monitoring the decrease in absorbance of the stabilized DPPH radical at 515 nm [7]. Briefly, 4 mg of DPPH was dissolved in 100 mL of methanol to prepare a 100 μM DPPH solution (initial absorbance ≈ 1.0). Each cured film (50 mg) was incubated in 3 mL of the DPPH solution in dark. The absorbance at 515 nm was recorded at 1 s intervals over a period of 120 min, using a DPPH solution without sample as the control. The radical scavenging activity (%) was calculated according to Eq. (4). Measurements were performed in triplicate, and the data represents the mean.

$$\text{Radical scavenging activity } (\%) = \frac{A_i - A_t}{A_i} \text{ x } 100 \quad (4)$$

where A_i is the absorbance of the control DPPH solution and A_t is the absorbance of DPPH solution incubated with the sample at a given time.

3. Results and discussion

3.1. Preparation of tri-eugenol-based isocyanurate (TEG)

The reaction between HDI-isocyanurate trimer and eugenol proceeded straightforward, affording the triallyl isocyanurate monomer (TEG) via urethane linkage formation. The reaction progress was monitored by ATR-FTIR, as shown in Fig. 1. The characteristic asymmetric stretching band of the isocyanate group (–NCO) at 2260 cm^{-1} nearly disappeared after 12 h, indicating almost complete consumption

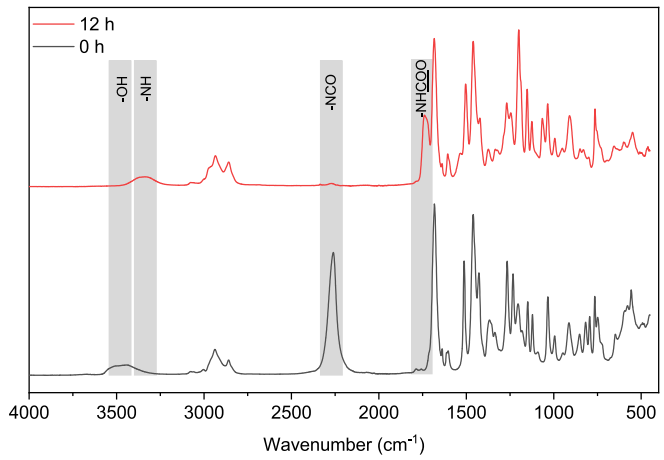

Fig. 1. Monitoring the reaction of HDI-isocyanurate trimer and eugenol via ATR-FTIR showing the formation of tri-eugenol based isocyanurate (TEG).

of the isocyanate groups. Quantitative analysis of the ATR-FTIR spectrum reveals that the conversion of isocyanate groups to urethane linkages reaches 98%. Furthermore, the hydroxyl (O—H) absorption band of eugenol at 3475 cm^{-1} diminished, while a new absorption band corresponding to urethane N—H stretching appeared at 3355 cm^{-1}. Additionally, a strong band at 1739 cm^{-1} emerged, attributable to the urethane C═O stretching vibration, further confirming the successful conjugation of eugenol through urethane bond [36].

The successful synthesis of TEG was further confirmed by ^{1}H NMR as shown in Fig. 2. Particularly, the aromatic protons signals of TEG exhibited a slight downfield shift relative to those of the parent eugenol, moving from 6.74 and 6.92 ppm to 6.77 and 7.03 ppm, respectively. Moreover, the signal of phenolic hydroxyl group at 5.70 ppm was almost vanished in the TEG spectrum. The conversion was determined by ^{1}H NMR, by integrating the residual phenolic hydroxyl group signal of unreacted eugenol. The conversion is approximately 95%, which is in excellent agreement with the value obtained from ATR-FTIR analysis (98%).

3.2. Thiol-ene photopolymerization of TEG-based networks

The thiol-ene click reaction of the tri-eugenol based isocyanurate (TEG), a trifunctional allyl, with either a trifunctional or tetrafunctional thiol (3SH or 4SH) was carried out under UV irradiation in the presence of 1 wt% BAPO as the photoinitiator (Scheme 2). In addition to the TEG-3SH and TEG-4SH formulations, in which the phenolic hydroxyl group of eugenol was consumed during urethane formation of TEG, two further formulations (TEG-EG-3SH and TEG-EG-4SH) were prepared by incorporating free eugenol. The latter afforded networks containing pendant phenolic hydroxyl groups, designed to impart antioxidant properties as discussed latter. For all systems, the stoichiometric thiol-to-ene ratio was maintained at 1:1, as summarized in Table 2. The photopolymerization kinetics were monitored by real-time FTIR spectroscopy. Prior to UV irradiation, the characteristic absorption bands of allyl (C=C) and thiol (S—H) groups are observed at 1639 and 2570 cm^{-1}, respectively (Fig. 3a). Upon UV exposure, both bands decreased progressively, reaching a plateau after approximately 2 min of UV irradiation. Thiol

Table 2
Photo-DSC analysis of UV cured TEG-based networks at 25 °C.

Entry	h_{peak}(W/g)	t_{peak} (*sec*)	ΔH_{exp} (J/g)
TEG-3SH	8.77	5	98
TEG-4SH	8.49	6	110
TEG-EG-3SH	5.25	6	94.57
TEG-EG-4SH	4.89	7	89.26

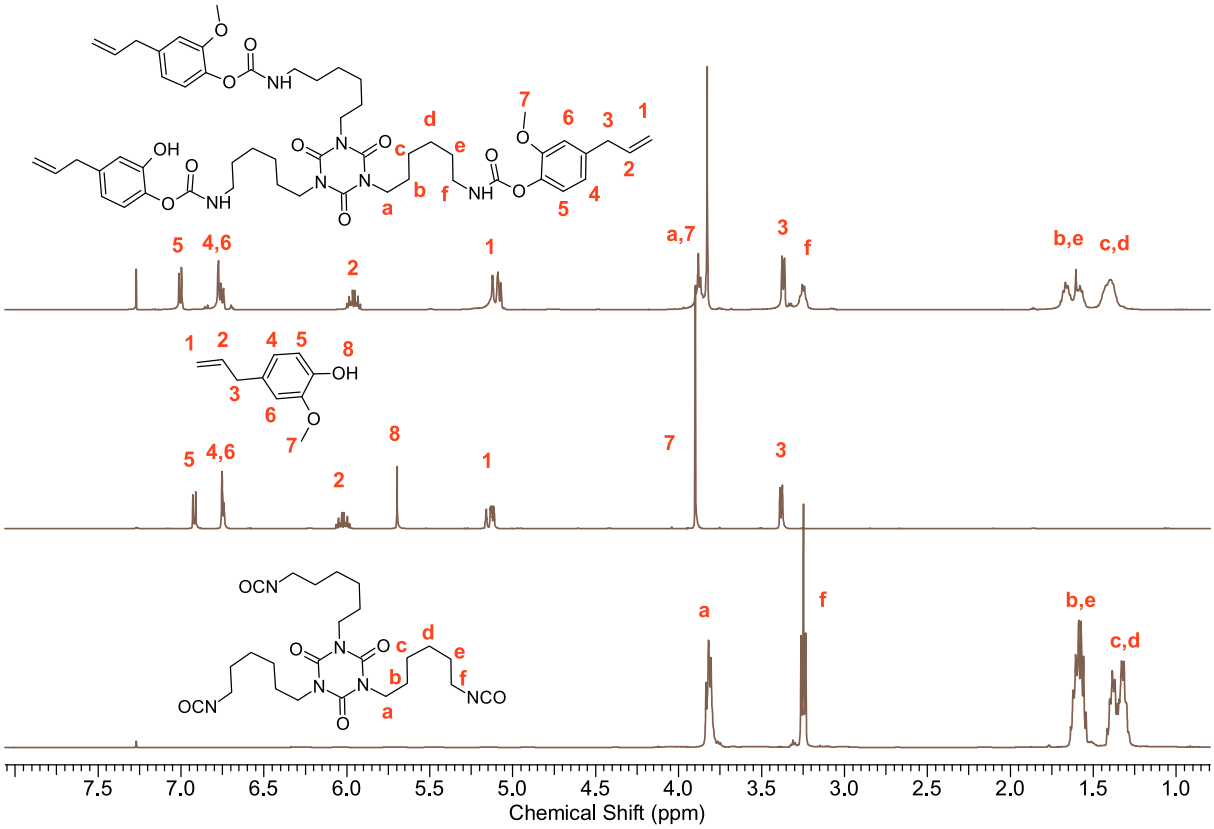

Fig. 2. ^{1}H NMR spectra of HDI-isocyanurate trimer, eugenol, and TEG in $CDCl_3$.

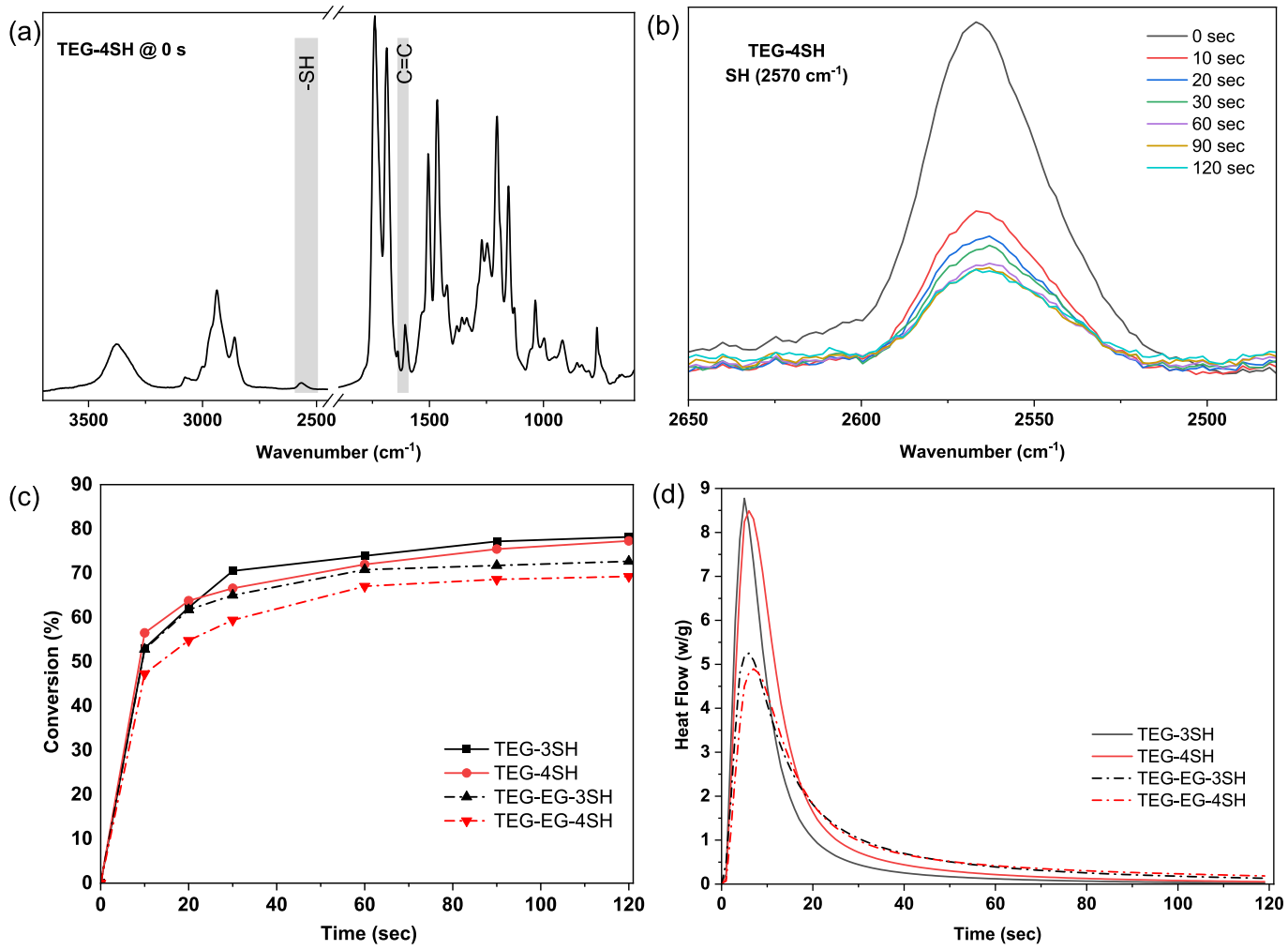

Fig. 3. Thiol-ene photopolymerization kinetics of TEG-based networks: (a) full FTIR spectrum of TEG-4SH before UV irradiation, (b) real-time FTIR spectra of TEG-4SH during UV irradiation exploring the decrease in the band intensities of thiol group, (c) conversion of thiol groups against UV irradiation time, (d) photo-DSC thermogram of UV-cured TEG-based networks at 25 °C.

group conversion, calculated from the decrease in the integrated -SH peak area as a function of irradiation time, is shown in Figs. 3b, c and S1. After 2 min, all formulations achieved high ultimate conversions in the range of 69–78%, confirming efficient thioether networks formation. Notably, formulations containing free eugenol (TEG-EG-3SH and TEG-EG-4SH) exhibited lower conversions compared to their eugenol-free analogue (TEG-3SH and TEG-4SH). This reduction is attributed to the radical scavenging effect of pendant phenolic hydroxyl groups, which compete with the propagation process during photopolymerization [37]. Additionally, the tetrafunctional thiol formulations consistently showed slightly lower conversions than those with the trifunctional thiol, likely due to increased steric hindrance associated with the higher thiol functionality [17,35].

Complementary photo-DSC measurements provided further insights into photopolymerization rate of these formulations (Fig. 3d and Table 3). The TEG-based networks without free eugenol (TEG-3SH and TEG-4SH) exhibited higher peak heat flow values (h_{peak}, 8.49–8.77 W/g) and greater total reaction enthalpies (ΔH, 98–110 J/g) compared to the eugenol-containing networks (4.89–5.25 W/g; 89–95 J/g). The presence of pendant phenolic hydroxyl groups in TEG-EG-3SH and TEG-EG-4SH markedly retarded polymerization rate, as evidenced by lower h_{peak} values and slightly delayed t_{peak}, consistent with the results observed by the real-time FTIR [38,39]. In particular, incorporation of free eugenol led to an approximate 40% reduction in h_{peak} and a decrease in total reaction enthalpies (ΔH), indicating a significant suppression of the polymerization rate and a slower overall network formation. Despite this retardation, all formulations ultimately reached high conversions after 2 min of UV irradiation, demonstrating that efficient photopolymerization can still be achieved while incorporating antioxidant functionality.

Table 3
Glass transition temperature (T_g), crosslinking density (ν) and gel content of UV cured TEG-based networks.

Entry	$T_{g,\ DSC}$ (°C)	$T_{g,\ DMA}$ (°C)	ν (mol/m^3)	Gel content (%)
TEG-3SH	19	34	460	97
TEG-4SH	21	38	840	95
TEG-EG-3SH	4	16	210	94
TEG-EG-4SH	6	25	360	93.5

Additionally, the gel content measurements (Table 4) revealed high values for all TEG-based networks, indicating that a large fraction of the material is insoluble as a result of extensive crosslink formation. This high gel fraction confirms the efficiency of the photopolymerization process and the successful formation of densely crosslinked, chemically stable thiol-ene networks.

3.3. Thermomechanical properties

Dynamic mechanical analysis (DMA) was employed to investigate

Table 4
Mechanical properties of TEG-based thiol-ene networks.

	Young's modulus	Ultimate stress	Ultimate strain	Stress at break	Strain at break
	E_t (MPa)	σ_M (MPa)	ε_M (%)	σ_B (MPa)	ε_B (%)
TEG-3SH	7.37 ± 0.48	2.69 ± 0.29	47.20 ± 3.52	1.72 ± 0.22	47.39 ± 5.25
TEG-4SH	54.34 ± 9.62	4.87 ± 0.64	56.14 ± 3.67	2.89 ± 0.31	56.96 ±2.11
TEG-EG-3SH	1.23 ± 0.31	0.70 ± 0.11	62.61 ± 5.55	0.42 ± 0.05	56.79 ± 6.51
TEG-EG-4SH	5.95 ± 0.56	2.36 ± 0.17	56.17 ± 3.89	1.43 ± 0.14	58.69 ± 3.82

the viscoelastic properties and crosslinking density of the UV-cured TEG-based networks. Fig. 4a presents the storage modulus (E′) and tan δ curves as a function of temperature for the four formulations. At 25 °C, the E′ values of TEG-4SH, TEG-3SH, TEG-EG-4SH, and TEG-EG-3SH are 312, 204, 25, and 3.6 MPa, respectively. These results clearly indicate that the tetrafunctional thiol produced more rigid networks compared to the trifunctional thiol, while the incorporation of eugenol as mono-allyl (TEG-EG-3SH and TEG-EG-4SH) led to a dramatic decrease in storage modulus, consistent with the expected reduction in crosslink density [18,35].

Crosslinking density (ν) was calculated from the rubbery plateau modulus (E′ at T_g + 40 °C) according to the theory of rubber elasticity (Table 4). As anticipated, the TEG-4SH formulation exhibits the highest crosslink density (840 mol m^{-3}), reflecting the greater number of reactive sites, whereas TEG-EG-3SH displays the lowest value (210 mol m^{-3}), due to both the reduced thiol functionality and the dilution of network connectivity by free eugenol [17].

The glass transition temperature (T_g) was determined from the peak temperature of the tan δ curves, yielding $T_{g,DMA}$ values of 38, 34, 25, and 16 °C for TEG-4SH, TEG-3SH, TEG-EG-4SH, and TEG-EG-3SH, respectively. These values follow the same trend as crosslinking density, confirming the strong correlation between network connectivity and T_g. Complementary DSC measurements (Fig. 4b) further supported these results, showing consistent T_g values across the four networks. Overall, the data demonstrate that both thiol functionality and crosslinking density are the key parameters governing the T_g of these thiol-ene networks. As is typical, thiol-ene systems exhibit relatively low T_g values due to the inherent flexibility of thioether linkages [40]. However, it is noteworthy that the T_g values of TEG-4SH and TEG-3SH are significantly higher than those of previously reported bio-based thiol-ene networks [41–44]. This enhancement can be attributed to the presence of rigid isocyanurate ring in the TEG backbone, which promote intermolecular

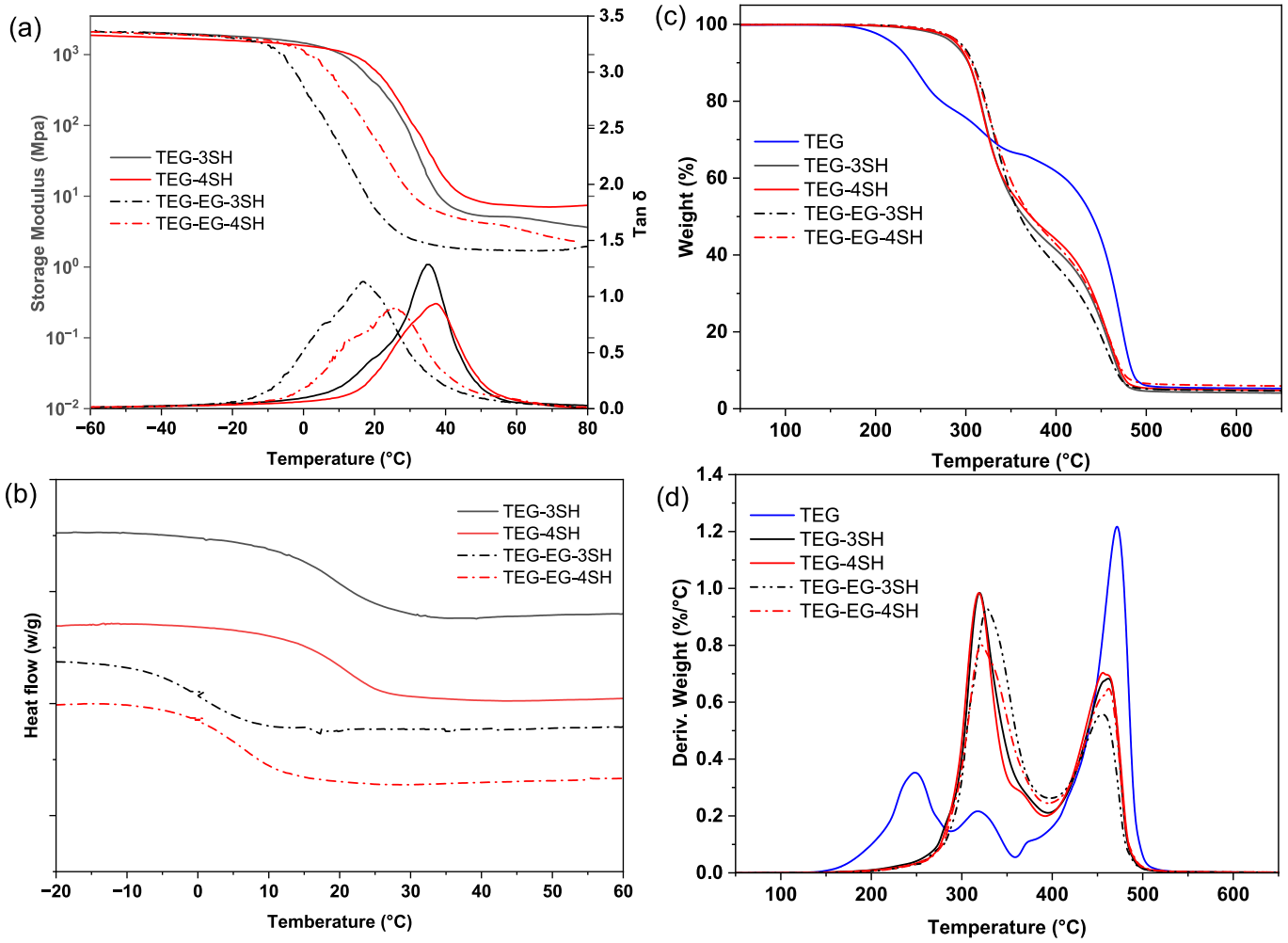

Fig. 4. Thermomechanical properties and thermal stability of TEG-based networks: (a) DMA curves of storage modulus (E') and tan δ against temperature; (b) DSC thermogram, (c) TGA, and (d) DTA curves.

hydrogen bonding and restrict chain mobility, thereby elevating the glass transition temperature.

The thermal stability of the tri-eugenol-based isocyanurate (TEG) precursor and the corresponding TEG-based thiol-ene networks were evaluated by thermogravimetric analysis (TGA) under a nitrogen atmosphere. The TGA and derivative thermogravimetric (DTG) curves are presented in Fig. 4c and d, and the degradation temperatures are summarized in Table S1. The thermogram of TEG demonstrates excellent thermal stability, with an initial 5% weight loss temperature ($T_{5\%}$) of approximately 220 °C and a final decomposition temperature (T_{final}) near 550 °C. Three distinct decomposition stages are evident: the peak decomposition temperature T_{max} of the first and second stages, centered at 250 °C and 320 °C with a combined weight loss of about 33%, correspond to urethane bond cleavage and volatilization of eugenol moieties. The third stage, with a maximum degradation rate at 470 °C, is attributed to decomposition of the isocyanurate ring structure, known for its aromatic-like thermal robustness [45,46].

Upon crosslinking with multifunctional thiols, all TEG-based networks exhibited significantly enhanced thermal stability, as indicated by elevated $T_{5\%}$ values in the range of 286–294 °C. The thermograms of these crosslinked systems displayed two dominant degradation stages. The first stage, with T_{max} around 320 °C and approximately 60% weight loss, is mainly associated with the thermal degradation of urethane linkages and the main structure of thiol crosslinkers [41]. The second stage, appearing at T_{max} of 460 °C and extending to 525 °C with a cumulative mass loss of about 95%, corresponds to the decomposition of the thermally stable isocyanurate ring. These results confirm that incorporation of the isocyanurate moiety effectively enhances the thermal stability of the resulting eugenol-based thiol-ene networks.

3.4. Mechanical properties

For applications in flexible polymeric materials, achieving an optimal balance between mechanical strength and flexibility is essential. As shown in Fig. 5, the digital photographs of the TEG-based networks demonstrate that TEG-based thiol-ene film can be freely bent without fracture, confirming their excellent flexibility. The stress-strain curves of TEG-based networks are presented in Fig. 5 and corresponding mechanical parameters are summarized in Table 4. Among the formulations, TEG-4SH displayed the highest stiffness ($E_t = 54.3 \pm 9.6$ MPa) and tensile strength ($\sigma_M = 4.87 \pm 0.64$ MPa; $\sigma_B = 2.89 \pm 0.31$ MPa), in line with its superior crosslinking density derived from the tetra-functional thiol structure. In comparison, TEG-3SH exhibited moderately lower modulus ($E_t = 7.37 \pm 0.48$ MPa) and strength ($\sigma_M = 2.69 \pm 0.29$ MPa), reflecting the reduced connectivity associated with the tri-thiol system [41,42]. In contrast, incorporation of free eugenol in formulation substantially diminished both modulus and strength, particularly in TEG-EG-3SH ($E_t = 1.23 \pm 0.31$ MPa; $\sigma_M = 0.70 \pm 0.11$ MPa), due to the dilution of crosslinking sites and consequent reduction in network integrity. Consequently, the chain mobility is enhanced, leading to greater extensibility, as evidenced by the ultimate strain ($\varepsilon_M = 62.6 \pm 5.6\%$) observed for TEG-EG-3SH. All networks exhibited ductile behavior with failure strains in the range of 47–59%. Collectively, these results confirm that increasing thiol functionality reinforces stiffness and strength through enhanced crosslink density, whereas the incorporation of eugenol imparts improved flexibility and ductility at the expense of strength, consistent with the trends observed in dynamic mechanical and thermal analyses.

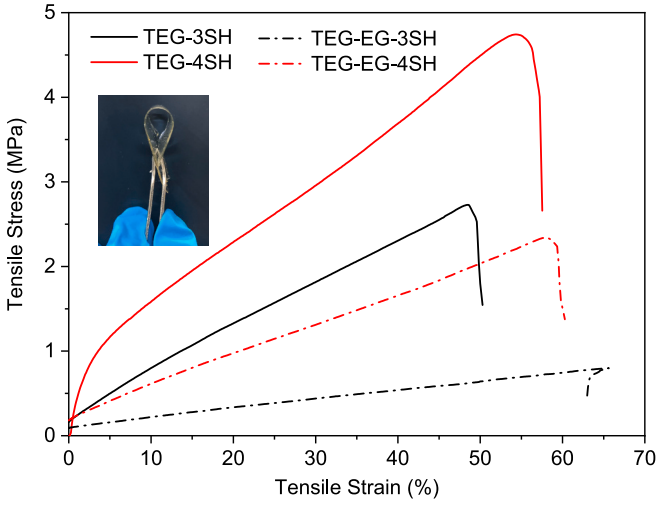

Fig. 5. Tensile stress-strain curves of TEG-based thiol–ene networks. The inset displays a photographic image illustrating the flexibility of the bent film.

3.5. Optical properties

The optical transparency of the TEG-based networks was evaluated by UV–Vis spectroscopy (Fig. 6). All formulations exhibited excellent transparency in the visible region. Specifically, the transmittance values above 500 nm exceeded 80% for all samples, consistent with the high optical clarity observed in the digital images (Fig. 6, inset). In contrast, the transmittance in the UV region (below 320 nm) approached zero, demonstrating the effective UV-shielding capability of these networks. The efficient UV-blocking behavior arises from the aromatic structure of the tri-eugenol units (TEG), which strongly absorb light in the medium- and short-wavelength UV region (Fig. S2) [17,47]. Taken together, these results confirm that the prepared bio-based thiol-ene networks combine successfully high optical clarity with effective UV-shielding properties. Such a combination is attractive for potential applications in optoelectronic devices, protective coatings, and biomedical materials, where both transparency and UV-blocking are critical [48,49].

3.6. Antioxidant activity

The antioxidant properties of the TEG-based thiol-ene networks (TEG-3SH, TEG-4SH, TEG-EG–3SH, and TEG-EG-4SH) were evaluated using the DPPH free radical scavenging assay, a widely employed method for assessing the radical scavenging capacity of polymeric materials. DPPH is a stable free radical characterized by a purple solution color and a distinct absorption band at 515 nm. Upon interaction with antioxidant moieties such as phenolic groups, DPPH abstracts a hydrogen atom, forming the reduced DPPH–H species, accompanied by

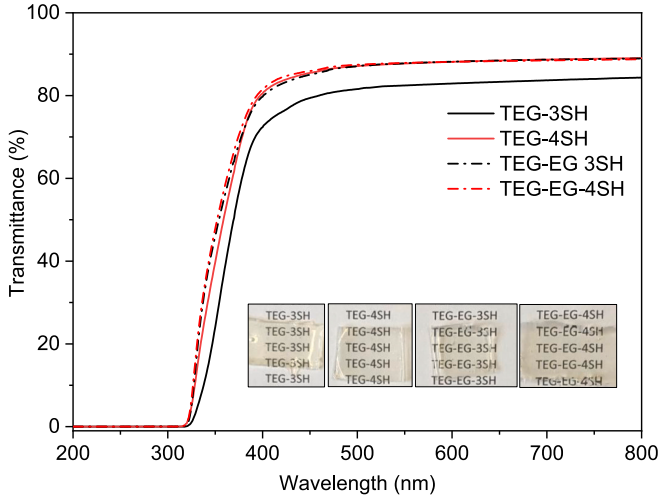

Fig. 6. UV–Vis spectra of TEG-based thiol-ene network films demonstrating high optical transmittance and effective UV-blocking properties. The inset presents a photographic image of the transparent films.

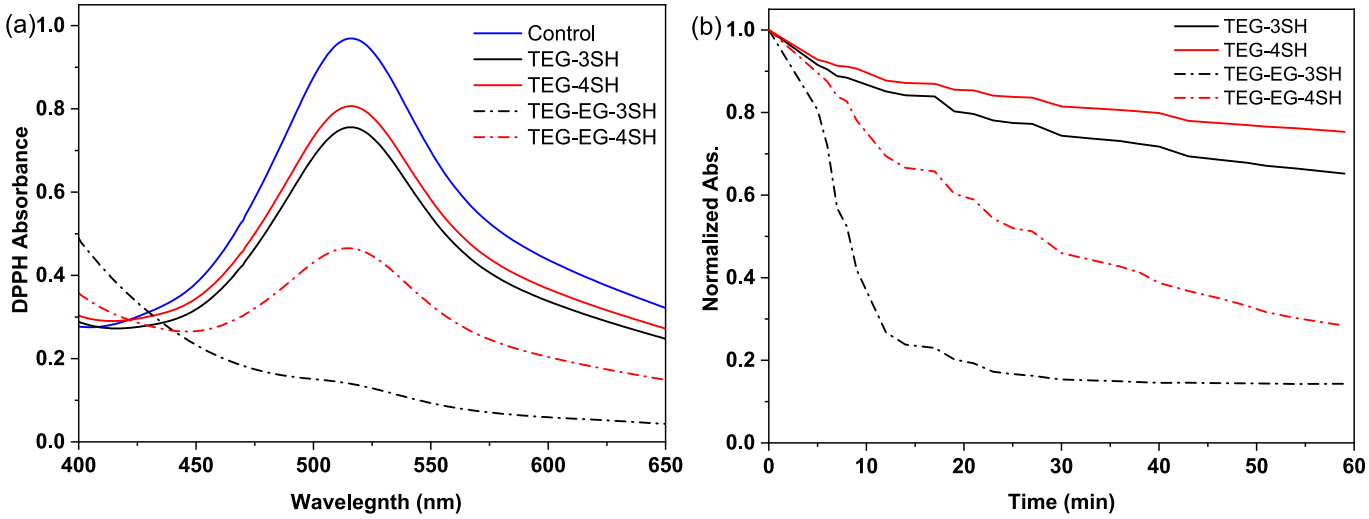

Fig. 7. (a) DPPH scavenging by different formulations of the TEG based thiol-ene networks after 15 min. (b) Time-dependant antioxidant activities.

a color change to yellow and a decrease in absorbance at 515 nm [7]. Fig. 7a shows the UV–Vis spectra of DPPH solutions after 15 min of incubation with 50 mg of the different TEG-based networks. As expected, TEG-3SH and TEG-4SH, which lack phenolic hydroxyl groups, displayed only marginal DPPH radical scavenging activity. This limited activity can be attributed to residual unreacted thiol groups, which are known to quench radicals through hydrogen transfer in addition to the limited activity of the thioether groups [6,50]. In contrast, the formulations contain mono-eugenol (TEG-EG-3SH and TEG-EG-4SH) exhibited pronounced radical scavenging activity, arising from the free phenolic hydroxyl groups incorporated into the networks [51]. Among these, TEG-EG-3SH demonstrated the highest scavenging efficiency (86%), consistent with its higher content of free phenolic groups (0.33 equiv. mol) compared to TEG-EG-4SH (52%), which contained only 0.25 equiv. mol. The time-dependent scavenging performance over 60 min is shown in Fig. 7b. TEG-EG-3SH achieved 58% scavenging after 10 min, which further increased to 86% at 60 min. In contrast, TEG-EG-4SH showed 22% scavenging at 10 min and gradually increased to 72% at 60 min. The relatively slower and lower scavenging capacity of TEG-EG-4SH can be attributed to both its reduced content of free phenolic groups and its higher crosslinking density, which hinders the diffusion of DPPH molecules into the polymer network. Overall, the incorporation of phenolic hydroxyl moieties into the thiol-ene networks imparts significant antioxidant functionality, thereby enhancing their potential for applications in areas where free radical scavenging is desirable, such as antimicrobial coatings, biomedical materials, and active packaging systems.

4. Conclusion

Eugenol based-isocyanurate thiol-ene networks are successfully fabricated via UV-initiated thiol-ene click chemistry, demonstrating a sustainable strategy for constructing multifunctional polymer networks. The incorporation of eugenol in formulations, either as a triallyl isocyanurate precursor (TEG) or in combination as free eugenol, enabled systematic control over crosslink density, thermal properties, and functional performance. Real-time FTIR and photo-DSC confirmed rapid photopolymerization and high thiol conversion within 2 min, while the presence of pendant phenolic hydroxyl groups induced a slight retardation due to radical quenching. The resulting networks exhibited excellent thermal stability, high optical transparency, and efficient UV-blocking. Mechanical and viscoelastic analyses revealed that increasing thiol functionality enhanced stiffness and T_g, whereas introduce of pristine eugenol imparted greater flexibility and ductility. Notably, formulations containing free phenolic groups showed pronounced intrinsic antioxidant activity, achieving up to 86% radical scavenging. Overall, this work presents a renewable approach for designing eugenol-based thiol-ene networks with tuneable mechanical behavior, thermal stability, UV-blocking, and antioxidant functionality, suitable for flexible coatings and protective polymeric materials.

CRediT authorship contribution statement

Mohamed Naguib: Writing – review & editing, Writing – original draft, Methodology, Investigation, Funding acquisition, Formal analysis, Data curation, Conceptualization. **Marco Sangermano:** Writing – review & editing, Investigation. **Mohamed A. Yassin:** Writing – review & editing, Writing – original draft, Methodology, Investigation, Formal analysis, Data curation, Conceptualization.

Declaration of competing interest

The authors declare that they have no known competing financial interests or personal relationships that could have appeared to influence the work reported in this paper.

Acknowledgments

Mohamed Naguib express his gratitude to the Academy of Scientific Research & Technology (ASRT, Egypt) for supporting the STARS-ASRT fellowship. The authors thank Ms. Kerstin Arnhold for carrying out TGA measurements (IPF Dresden) and Mr. Holger Scheibner for carrying out the tensile measurements

Appendix A. Supplementary data

Supplementary data to this article can be found online at https://doi.org/10.1016/j.reactfunctpolym.2026.106701.

Data availability

Data will be made available on request.

References

[1] S.B. Nimse, D. Pal, Free radicals, natural antioxidants, and their reaction mechanisms, RSC Adv. 5 (2015) 27986–28006.

[2] J. Brito, H. Hlushko, A. Abbott, A. Aliakseyeu, R. Hlushko, S.A. Sukhishvili, Integrating antioxidant functionality into polymer materials: fundamentals, strategies, and applications, ACS Appl. Mater. Interfaces 13 (2021) 41372–41395.
[3] A. Dhawan, V. Kumar, V.S. Parmar, A.L. Cholli, Novel polymeric antioxidants for materials, in: Antioxidant Polymers, 2012, pp. 385–425.
[4] H. Yamaguchi, M. Itoh, H. Ishikawa, K. Kusuda, Antioxidant activity of polymers bearing hindered phenolic groups, J. Macromol. Sci. A 30 (1993) 287–292.
[5] B. Xue, K. Ogata, A. Toyota, Synthesis and radical scavenging ability of new polymers from sterically hindered phenol functionalized norbornene monomers via ROMP, Polymer 48 (2007) 5005–5015.
[6] H. Kim, J. Lee, Y. Hong, C. Lim, D.W. Lee, D.X. Oh, J.H. Waite, D.S. Hwang, Essential role of thiols in maintaining stable catecholato-iron complexes in condensed materials, Chem. Mater. 34 (11) (2022) 5074–5083.
[7] M. Naguib, M.A. Yassin, Polymeric antioxidant via ROMP of bioderived tricyclic oxanorbornene based on vanillin and furfurylamine, ACS Appl. Polym. Mater. 4 (3) (2022) 2181–2188.
[8] D. Kai, M.J. Tan, P.L. Chee, Y.K. Chua, Y.L. Yap, X.J. Loh, Towards lignin-based functional materials in a sustainable world, Green Chem. 18 (2016) 1175–1200.
[9] S. Molina-Gutiérrez, A. Manseri, V. Ladmiral, R. Bongiovanni, S. Caillol, P. Lacroix-Desmazes, Eugenol: a promising building block for synthesis of radically polymerizable monomers, Macromol. Chem. Phys. 220 (2019).
[10] R. Morales-Cerrada, S. Molina-Gutierrez, P. Lacroix-Desmazes, S. Caillol, Eugenol, a promising building block for biobased polymers with cutting-edge properties, Biomacromolecules 22 (2021) 3625–3648.
[11] J. Zheng, Y. Cai, X. Zhang, J. Wan, H. Fan, Eugenol-based siloxane acrylates for ultraviolet-curable coatings and 3D printing, ACS Appl. Polym. Mater. 4 (2022) 929–938.
[12] Y. Hu, Y. Tian, J. Cheng, J. Zhang, Synthesis of eugenol-based polyols via thiol–ene click reaction and high-performance thermosetting polyurethane therefrom, ACS Sustain. Chem. Eng. 8 (2020) 4158–4166.
[13] I. Faye, M. Decostanzi, Y. Ecochard, S. Caillol, Eugenol bio-based epoxy thermosets: from cloves to applied materials, Green Chem. 19 (21) (2017) 5236–5242.
[14] B. Jiang, J. Ying, G. Chen, J. Han, S. Wang, S. Wu, S.-N. Li, L. Peng, S. Wu, Y. Guo, Eugenol-derived thiol–ene photopolymerization networks with exceptional flame retardancy, mechanical robustness, and chemical degradability, ACS Sustain. Chem. Eng. 13 (26) (2025) 10019–10028.
[15] O. Ozukanar, E. Çakmakçi, G. Sagdic, U.S. Gunay, H. Durmaz, V. Kumbaraci, Eugenol-DOPO: a bio-based phosphorous-containing monomer for thiol-ene photocurable thermosets, J. Polym. Environ. 31 (7) (2023) 3259–3271.
[16] O. Ozukanar, E. Çakmakçi, O. Daglar, H. Durmaz, V. Kumbaraci, Thiol-ene photopolymerization meets azide-alkyne click reactions: P/N/Si-containing, dual curable eugenol-based hybrid coatings, Eur. Polym. J. 195 (2023) 112203.
[17] T. Liu, L. Sun, R. Ou, Q. Fan, L. Li, C. Guo, Z. Liu, Q. Wang, Flame retardant eugenol-based thiol-ene polymer networks with high mechanical strength and transparency, Chem. Eng. J. 368 (2019) 359–368.
[18] Y. Tian, Q. Wang, J. Cheng, J. Zhang, A fully biomass based monomer from itaconic acid and eugenol to build degradable thermosets via thiol–ene click chemistry, Green Chem. 22 (3) (2020) 921–932.
[19] J.O. Akindoyo, M.H. Beg, S. Ghazali, M.R. Islam, N. Jeyaratnam, A. Yuvaraj, Polyurethane types, synthesis and applications–a review, RSC Adv. 6 (115) (2016) 114453–114482.
[20] D.K. Chattopadhyay, K. Raju, Structural engineering of polyurethane coatings for high performance applications, Prog. Polym. Sci. 32 (3) (2007) 352–418.
[21] M.S. Mahajan, P.P. Mahulikar, V.V. Gite, Eugenol based renewable polyols for development of 2K anticorrosive polyurethane coatings, Prog. Org. Coat. 148 (2020) 105826.
[22] X. Zhang, Y. Cai, X. Zhang, T. Aziz, H. Fan, C. Bittencourt, Synthesis and characterization of eugenol-based silicone modified waterborne polyurethane with excellent properties 138 (2021).
[23] S. Wendels, L. Avérous, Biobased polyurethanes for biomedical applications, Bioact. Mater. 6 (4) (2021) 1083–1106.
[24] M. Naguib, M.A. Yassin, M.A. Rehim, Antimicrobial polyurethane films based on quaternary ammonium salts functionalized soybean oil, Macromol. Chem. Phys. 224 (1) (2023) 2200231.
[25] J. Chambers, J. Jiricny, C.B. Reese, The thermal decomposition of polyurethanes and polyisocyanurates, Fire Mater. 5 (1981) 133–141.
[26] M. Modesti, A. Lorenzetti, Flame retardancy of polyisocyanurate–polyurethane foams: use of different charring agents, Polym. Degrad. Stab. 78 (2002) 341–347.
[27] R. Heath, Chapter 28 - isocyanate-based polymers: polyurethanes, polyureas, polyisocyanurates, and their copolymers, in: M. Gilbert (Ed.), Brydson's Plastics Materials, Eighth edition, Butterworth-Heinemann, 2017, pp. 799–835.
[28] C.E. Hoyle, C.N. Bowman, Thiol–ene click chemistry, Angew. Chem. Int. Ed. 49 (2010) 1540–1573.
[29] Y. Zhai, D. Zhang, L. Gao, Eugenol-based high-strength and toughness shape memory poly (urethane thioether) networks as intrinsic UV-shielding devices, Biomacromolecules 25 (9) (2024) 5949–5958.
[30] K. Ma, S. Zhao, H. Zhao, Y. Liu, Y. Fu, C. Pang, Biobased thiol-ene networks with high optical transparency and Abbe number derived from citric acid, Macromolecules 57 (2024) 7614–7623.
[31] A.L. Flourat, L. Pezzana, S. Belgacem, A. Dosso, M. Sangermano, S. Fadlallah, F. Allais, Levoglucosenone to 3D-printed green materials: synthesizing sustainable and tunable monomers for eco-friendly photo-curing, Green Chem. 25 (2023) 7571–7581.
[32] T. Touchet, S. Briggs, L. Graul, D.J. Maitland, Development and characterization of oxidatively responsive thiol–ene networks for bone graft applications, ACS Appl. Bio Mater. 5 (2022) 2633–2642.
[33] D. Moraru, B. Chícharo, G. Trapasso, S. Fadlallah, F. Allais, F. Aricò, M. Sangermano, Thiol-ene UV-cured biodegradable coatings from α,ω-diene furanic monomers 7 (2025) 2073–2079.
[34] L. Pezzana, M. Sangermano, Fully biobased UV-cured thiol-ene coatings, Prog. Org. Coat. 157 (2021) 106295.
[35] J.-T. Miao, L. Yuan, Q. Guan, G. Liang, A. Gu, Water-phase synthesis of a biobased allyl compound for building uv-curable flexible thiol–ene polymer networks with high mechanical strength and transparency, ACS Sustain. Chem. Eng. 6 (6) (2018) 7902–7909.
[36] H.-G. Oh, T.-U. Oh, S. Hong, S.-H. Cha, Synthesis and characterization of antibacterial self-healable biopolyurethanes with eugenol-based bio-polyol, Mater. Today Commun. 35 (2023) 106381.
[37] R. Ding, Y. Du, R.B. Goncalves, L.F. Francis, T.M. Reineke, Sustainable near UV-curable acrylates based on natural phenolics for stereolithography 3D printing, Polym. Chem. 10 (9) (2019) 1067–1077.
[38] L. Pezzana, R. Wolff, J. Stampfl, R. Liska, M. Sangermano, High temperature vat photopolymerization 3D printing of fully bio-based composites: green vegetable oil epoxy matrix & bio-derived filler powder, Addit. Manuf. 79 (2024) 103929.
[39] L. Pezzana, S. Fadlallah, G. Giri, C. Archimbaud, I. Roppolo, F. Allais, M. Sangermano, DLP 3D printing of levoglucosenone-based monomers: exploiting thiol-ene chemistry for bio-based polymeric resins, ChemSusChem 17 (22) (2024) e202301828.
[40] C. Resetco, B. Hendriks, N. Badi, F. Du Prez, Thiol–ene chemistry for polymer coatings and surface modification – building in sustainability and performance, Mater. Horiz. 4 (6) (2017) 1041–1053.
[41] P. Jia, M.E. Lamm, Y. Sha, Y. Ma, L.B. Kurnaz, Y. Zhou, Thiol-ene eugenol polymer networks with chemical degradation, thermal degradation and biodegradability, Chem. Eng. J. 454 (2023) 140051.
[42] J. Xue, X. Yang, Y. Ke, Z. Yan, X. Dong, Y. Luo, C. Zhang, Novel eugenol-based allyl-terminated precursors and their bio-based polymer networks through thiol-ene click reaction, Ind. Crop. Prod. 171 (2021) 113956.
[43] T. Yoshimura, T. Shimasaki, N. Teramoto, M. Shibata, Bio-based polymer networks by thiol–ene photopolymerizations of allyl-etherified eugenol derivatives, Eur. Polym. J. 67 (2015) 397–408.
[44] J. Dai, S. Ma, L. Zhu, S. Wang, L. Yang, Z. Song, X. Liu, J. Zhu, UV-thermal dual cured anti-bacterial thiol-ene networks with superior performance from renewable resources, Polymer 108 (2017) 215–222.
[45] A. Xiang, Y. Li, L. Fu, Y. Chen, H. Tian, A.V. Rajulu, Thermal degradation and flame retardant properties of isocyanate-based flexible polyimide foams with different isocyanate indices, Thermochim. Acta 652 (2017) 160–165.
[46] J. Jiricny, C.B. Reese, The thermal decomposition of isocyanurates, Br. Polym. J. 12 (3) (1980) 81–84.
[47] W. Yang, W. Zhou, N. Ding, S. Shen, D. Gao, D. Puglia, Y. Duan, P. Xu, T. Liu, Z. Wang, Biobased photothermal responsive shape memory polythioether/MXene nanocomposites with self-extinguishing performance, Chem. Eng. J. 497 (2024) 154591.
[48] A.F. Ghanem, M.A. Yassin, R. Cosquer, F. Gouanvé, E. Espuche, M.H.A. Rehim, Polycaprolactone composite films infused with hyperbranched polyester/reduced graphene oxide: influence on biodegradability, gas/water transport and antimicrobial properties for sustainable packaging, RSC Adv. 14 (9) (2024) 5740–5753.
[49] M.M. Elmahdy, M.A. Yassin, Linear and nonlinear optical parameters of biodegradable chitosan/polyvinyl alcohol/sodium montmorillonite nanocomposite films for potential optoelectronic applications, Int. J. Biol. Macromol. 258 (2024) 128914.
[50] J. Wang, S. Huang, K. Yan, J. Shi, S. Shi, Y. Jin, L. Yuan, Sustainable macromolecular antioxidants from eugenol with synergistically enhanced storage stability for active PVA packaging, React. Funct. Polym. 191 (2023) 105671.
[51] T. Modjinou, D.-L. Versace, S. Abbad-Andallousi, N. Bousserrhine, P. Dubot, V. Langlois, E. Renard, Antibacterial and antioxidant bio-based networks derived from eugenol using photo-activated thiol-ene reaction, React. Funct. Polym. 101 (2016) 47–53.